JOURNAL OF CATALYSIS 133, 1–20 (1992)

Vanadia Supported on TiO_2–SiO_2 Mixed Oxide Gels: Structure of the Dispersed Phase and Activity for the Selective Catalytic Reduction of NO with NH_3

BRENT E. HANDY,* ALFONS BAIKER,*,[1] MATTHIAS SCHRAML-MARTH,† AND ALEXANDER WOKAUN†

*Department of Chemical Engineering and Industrial Engineering, Swiss Federal Institute of Technology, ETH-Zentrum, CH-8092, Zurich, Switzerland; and †Physical Chemistry II, University of Bayreuth, D-W-8580 Bayreuth, Germany

Received February 26, 1991; revised June 4, 1991

Supported vanadia catalysts were prepared by reacting vanadyl triisopropoxide with titania–silica mixed oxide supports of fixed Ti : Si mol ratio (1 : 4 and 1 : 1), but of varying pore structure, surface area, and crystallinity. The latter properties were controlled by varying the sol-gel preparation parameters. Although the selectivity pattern for the selective catalytic reduction (SCR) remained essentially the same over all catalysts, the specific activity, defined on a per V^{5+} basis, varied with the support. The vanadia content in all catalysts corresponded to less than one monolayer (defined as 0.10 wt% $V_2O_5m^2$ or 11 μmol V^{5+}/m^2), and structural data indicate that the vanadia is well dispersed. Raman spectroscopy was used to differentiate between vanadia species immobilized on TiO_2 and SiO_2 domains, respectively. These results revealed that the mixed oxide gels can be categorized into two main types exhibiting titania- or silica-like behavior. A weak interaction that results from a two-stage hydrolysis procedure of the alkoxide precursors of the constituents is characteristic for silica-like supports. This contrasts with the titania-like behavior observed for TiO_2–SiO_2 mixed oxides prepared by single-stage hydrolysis, where the vanadia–support interaction is strong. No crystalline V_2O_5 phases were detected. TPR profiles show that the reducibility of vanadia, as evidenced by shifts in the temperature of maximum hydrogen consumption, is dependent upon the composition and preparation method of the mixed gel supports. An increase in the value of T_{max} can be correlated with a decrease in the turnover frequency (NO converted per V^{5+} site) of the SCR reaction.

INTRODUCTION

In the search for new catalysts for the selective catalytic reduction (SCR) of NO with NH_3, titania-supported vanadia catalysts have been found to be favorable due to their high activity at low temperatures (350–650 K), high selectivity for reduction to N_2 with minimal N_2O production, and good resistance to poisoning by SO_2, which is often present in stack emissions (*1*). Silica-supported vanadia catalysts were found to be less active than V/TiO_2, requiring a higher vanadia content to achieve similar NO conversion as titania- or alumina-supported catalysts (*2, 3*). However, it has been shown that the deposition of vanadia on SiO_2–TiO_2 can lead to improved SCR catalysts (*2–6*). Shikada *et al.* (*2*) and Odenbrand *et al.* (*4*) prepared silica-based catalysts by first producing a SiO_2–TiO_2 coprecipitate by homogeneously raising the pH of an acidified solution of Na_2SiO_3 and $TiCl_4$ using the hydrolysis of urea. A 50/50 (w/w) TiO_2–SiO_2 support, prepared by a homogeneous precipitation method, was impregnated with a solution of NH_4VO_3 to produce a catalyst that achieved the same level of NO conversion as V/SiO_2 and V/Al_2O_3 catalysts, but at 50–100 K lower temperature (*5*). Vogt *et al.* (*6*) describe a preparation technique for V_2O_5/TiO_2–SiO_2 catalysts

[1] To whom correspondence should be addressed.

0021-9517/92 $3.00

suitable for SCR. The addition of a uniform interlayer of titania was achieved by subsequent precipitation of hydrated titanium(III) and vanadium(III) oxides onto silica.

Physical and chemical properties of supported vanadia layer catalysts have been reviewed very recently by Bond and Flamerz (*7*). These properties are mainly influenced by the vanadia loading and the nature of the support. Using a grafting method (*8*), Baiker *et al.* (*9*) reported increases in NO turnover per V^{5+} site with successive graftings of a pure titania support. This has been attributed to the buildup of disordered "submonolayer" structures of vanadia with increasing layer number, first by reaction of the vanadyl precursor molecule with support hydroxyl groups, then including reaction with secondary hydroxyls on the V-moieties, generated by a mild oxidation treatment between graftings to remove organic groups. The submonolayer region has been defined (*10*) as <0.10 wt% V_2O_5 per m^2 of available titania area, which corresponds to 11 μmol V^{5+} per m^2. Provided that sufficient interaction with the support exists in this range of loading, vanadia should be 100% accessible for reaction. In previous work with the V-grafted catalyst on pure titania, the product selectivity of the dispersed vanadia is unchanged relative to bulk vanadia (*9, 11*).

In V-grafted mixed gel SiO_2–TiO_2 supports (*3*), a single application of vanadyl triisopropoxide precursor is sufficient to achieve a high NO turnover per V^{5+} site at a minimum of vanadia content. Furthermore, the activity was found to vary with the TiO_2 content of the gels. Structurally, the gels consisted of small anatase domains in an amorphous silica matrix, and the degree of mixing of both components is probably higher than by conventionally prepared mixed oxide preparations. Temperature-programmed reduction (TPR) results of the V-grafted gels (*3*) show evidence for a single vanadia phase, the reducibility of which is dependent upon the TiO_2 content of the gel support.

In this study, the chemical and structural nature of the dispersed vanadia on V-grafted mixed SiO_2–TiO_2 gel supports is investigated, using primarily supports of the same TiO_2 content (Ti : Si = 1.4), but different pore structure, surface area, and crystallinity, as achieved through variation of sol-gel processing conditions (*12*) to observe any influences of these properties on the active vanadia component.

EXPERIMENTAL

Catalyst Preparation

Using sol-gel principles, mixed oxide gels were prepared from the hydrolysis of tetraethoxy orthosilicate (TEOS) and tetraisopropoxy orthotitanate (TIOT). Altogether, seven TiO_2–SiO_2 mixed gel supports with a Ti : Si mol ratio of 1 : 4 and one support with a 1 : 1 mol ratio were used to make catalysts. The preparation of these gels and pore structural information are described in detail elsewhere (*12*) and are also available from the authors on request. Briefly, in five supports (labels, C, D, E, F, and G) three sol-gel parameters, namely, (i) pH of TEOS hydrolysis, (ii) complete or stagewise hydrolysis with component addition, and (iii) aging of several mixed gels (in dried or undried form) in slightly basic medium, were varied to produce different gel structures. The hydrolysis of TEOS was performed in either acidic medium (1 *M* HCl) or basic medium (ammonia water adjusted to pH 9). Gel H was prepared by mixing a dispersion of Aerosil 200 (Degussa AG), predried at 393 K, in excess isopropanol with TIOT in 1 : 4 Ti : Si ratio. After allowing components to mix thoroughly, hydrolysis was effected with slow addition of alcohol diluted 1 *M* HCl. Gels A and B, of 1 : 4 and 1 : 1 Ti : Si content, respectively, are similar to those described in Ref. (*10*). TEOS was hydrolyzed by vigorous stirring in excess distilled water for 20 h and the resulting silica sol combined with titania sol was made by slow addition of TIOT (diluted 1 : 1 in isopropanol) to an excess of 1 *M* HCl. A summary of the catalysts together with some characteristic properties of them are listed in Table 1.

Thermal and oxidative treatments of sup-

TABLE 1

Vanadia Grafted on TiO_2–SiO_2-mixed oxide gel catalysts: Composition, Textural Properties, and TPR Data

No. of V grafts	Gel	Ti : Si mol ratio	XRD	SA[a] (m^2/g)	H_2 Cons. (mmol/g)	T_{max}[b] (K)	wt% V_2O_5
1	A	1 : 4	Small anatase domains	362	0.51	780 (805)	4.7
2	A	1 : 4	Small anatase domains	(326)	1.21	809 (803)	11.0
3	A	1 : 4	Small anatase domains	289	1.37	828 (822)	12.5
1	B	1 : 1	Small anatase domains	228	0.34 ± .02	763	3.1
2	B	1 : 1	Small anatase domains	(218)	0.70	775	6.4
3	B	1 : 1	Small anatase domains	208	1.27 ± .08	785	11.6
1	C	1 : 4	Anatase; rutile (20%)	151	0.32	815 (773,738)	2.9
1	D	1 : 4	Small anatase domains	295	0.46	810	4.2
2	D	1 : 4	Small anatase domains	275	0.87	826	7.9
3	D	1 : 4	Small anatase domains	260	1.07	833	9.7
1	E	1 : 4	Anatase; rutile (20–30%)	309	0.60	819	5.4
1	F	1 : 4	Amorphous	454	0.59	884	5.3
1	G	1 : 4	Amorphous	71	0.21	863	1.9
1	H	1 : 4	V. small anatase domains	174	0.30	774	2.7
2	H	1 : 4	V. small anatase domains	(165)	0.57	783 (812)	5.1
3	H	1 : 4	V. small anatase domains	156	0.85	791	7.7
1	SiO_2	—	Amorphous	612	0.51	817	4.6

[a] Surface area (SA) values in parentheses are arithmetic mean of 1V and 3V values.
[b] Shoulder and other minor peaks listed in parentheses, in order of prominence.

ports and catalysts were performed with flowing nitrogen and oxygen streams (99.999%) with moisture removed by activated molecular sieve traps. Dry hexane was used as the solvent (Fluka Puriss, molecular sieve dried). The supports were impregnated with vanadium by the "grafting" method of reaction between vanadyl triisopropoxide (Alfa Products, Inc., ~98%) and the support surface hydroxyl groups. Prior to impregnation, 5 g of the support (0.3–0.5 mm size fraction) were precalcined in oxygen for 1 h at 870 K, followed by 2 h in nitrogen before cooling under flow to ambient. The support was then transferred under nitrogen to a purged and dried glass reaction flask immersed in an oil bath. A solution containing 1 ml of the vanadyl precursor in 20 ml hexane was injected into the flask and the contents maintained at 323–325 K (oil bath temp 343 K) for 12 h. The solution was then decanted, and the sample was washed three times with fresh hexane and dried under nitrogen flow, the flask remaining immersed in the oil bath. The sample was transferred back to the quartz treatment tube and activated by first heating in nitrogen to 573 K to degas the surface; then it was cooled back to ambient before switching to oxygen flow and reheated to 573 K, with this temperature maintained for 3 hours.

Catalyst Characterization

Catalysts were characterized by powder X-ray diffraction, nitrogen adsorption (BET) TPR, and Raman spectroscopy. TPR runs were performed under the following conditions: sample weight, 0.1–0.3 g, 5% H_2/Ar at 75 ml/min, heating rate, 10 K/min. Prior to each TPR run, the samples were oxidized *in situ* at 573 K.

For recording the Raman spectra the catalyst powders were pressed into self-supporting, nontransparent disks of 12-mm diameter, to avoid any perturbation due to scattering from quartz cell material. The 488-nm line of an argon-ion laser (Spectra Physics, Model 2025-05) was used to excite

the sample. Plasma lines from the laser were eliminated with a filter monochromator (Applied Photophysics, Model 2300).

It is known (*13, 14*) that the structure of the surface vanadia species strongly depends upon the hydrous state of the surface. As SCR reactions are normally run at temperatures higher than ambient, we are interested in the structure of the surface vanadia species under dehydrated conditions. To prepare this condition, Raman spectra have been excited at the comparatively high laser power of 100 mW. Operating at high laser powers leads to removal of surface water and to condensation of free hydroxyl groups, either from the support surface or as "secondary" OH-groups from surface vanadia (*15*), such that the state of our surface can be regarded as dehydrated. The spectra recorded did not exhibit any time dependence indicating stable dehydrated conditions.

Scattered light was collected and dispersed using a double monochromator (SPEX, Model 14018). For detection of the Raman signals, a cooled RCA-C31034A-02 GaAs photomultiplier tube was used. The slit width of the monochromator was adjusted to correspond to a spectral resolution of 2 cm^{-1}.

Catalytic Tests

Catalyst testing for the selective catalytic reduction of NO with NH_3 was performed in a 6-mm-o.d. quartz tube reactor with on-line mass spectrometric analysis of reactant and product gases. The reactor setup and mass spectrometric analysis methods are described in detail elsewhere (*16*). Feed gas concentrations were 900 ppm NO and NH_3, 18,000 ppm O_2, in a balance of argon. The reactor bed consisted of 0.1 g of 0.3- to 0.5-mm granules. Routine testing involved an integral test and a differential test. In the former, the product yields of N_2 and N_2O were studied by increasing catalyst temperature at a constant space velocity of 24,000 GHSV. Differential testing was performed in the 370–570 K range while maintaining conversion at 20% or lower.

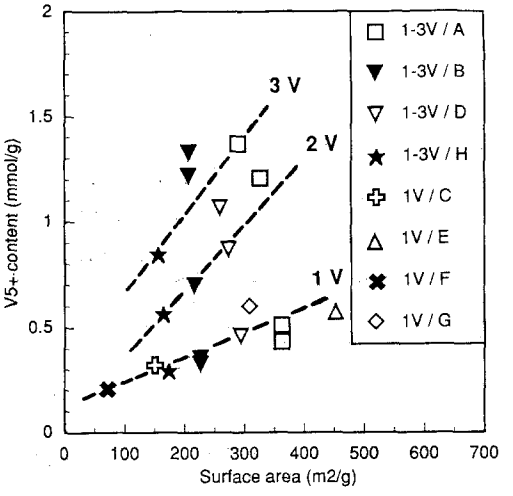

FIG. 1. Vanadia content, determined from hydrogen consumption during temperature-programmed reduction (TPR), as a function of gel surface area.

RESULTS

Grafting of Supports with the Vanadyl Precursor

During contact between support powder and the precursor solution, a surface reaction occurs (*8*) according to

$$\text{support–OH} + \text{VO}(OR)_3 \rightarrow \text{support–O–VO}(OR)_2.$$

The support pretreatment at 870 K presumably removes most of the surface hydroxyl sites present at lower temperatures, and vanadia content varies directly to available surface area, as shown in Fig. 1. Lines corresponding to one-, two-, and threefold graftings are superimposed on the data. For the first grafting, the slope corresponds to a vanadia site density of 0.6 V^{5+} per nm^2 and, for the second and third graftings, to 1.6 and 2.6, respectively. Note that a monolayer coverage defined as 0.10 wt% V_2O_5/m^2 (*10*) corresponds to 6.6 V^{5+}/nm^2. The surface area diminishes by 10–15% as the loading of vanadia increases. This behavior may be due to the buildup of the vanadia layer in the smallest mesopores and/or to structural changes occurring during the heat treatments between successive impregnations. Few support surface hydroxyls will be avail-

able for the initial grafting, and this is reflected in the low site density of singly grafted supports. As determined from *in situ* IR studies of the grafting process on pure titania, the support hydroxyl groups are totally consumed during the grafting process (*15*). The vanadia deposition per grafting is higher in second and third graftings. Because of the lower temperature used in calcining the grafted support, moisture evolved during the oxidation of the alcoholate groups will rehydroxylate bare support surface, in addition to generating secondary hydroxyl sites on the vanadyl surface complexes. Thus, both types of hydroxyls can serve as anchoring sites for the next grafting step. From previous grafting experiments with pure titania support (*9, 11*) it was apparent that successive graftings lead to a steady buildup of vanadia until the fourth grafting, after which the vanadia content is steady, and the surface presumably saturated with disordered, but interlinked vanadia moieties.

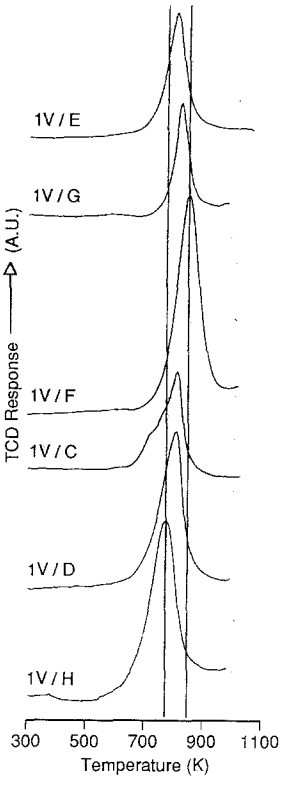

FIG. 2. Temperature-programmed reduction profiles of several mixed oxide gel supports singly grafted with vanadyl alkoxide precursor.

The Reducibility of the Vanadia Layer

TPR profiles of the singly grafted supports are presented in Fig. 2. To ensure that the vanadia was present as V_2O_5 at the start of the TPR runs, the samples were oxidized in air at 573 K for 3 hours prior to the TPR runs, which were then carried out *in situ*, i.e., without exposure of the sample to atmosphere. The amount of vanadium(V) species was calculated from the hydrogen consumptions determined in the TPR experiments assuming that on all catalysts reduction of vanadium(V) to vanadium(III) occurred. The validity of the latter assumption was confirmed for several samples by comparing the hydrogen consumptions with quantitative analysis of the vanadia using X-ray fluorescence (XRF) and inductive coupled plasma (ICP) analysis.

On all gels except for gel C, reduction is evidenced by a single peak. Peak halfwidths are about 50 K, and the differences in the position of the peak maximum temperature are observed, ranging for all gel catalysts of 1 : 4 Ti : Si content from 774 K, for 1V/H, to 884 K for 1V/F. Thus, despite differences in the pore structure and crystallinity of these gel supports (*12*), the chemical nature of the surface structure, at least in the vicinity of the vanadia layer, is homogeneous, as judged from TPR measurements. Multiple reduction peaks suggest several types of vanadia structures in 1V/C, although the majority species lie under the peak centered at 815 K. Assuming a similar peak halfwidth for all peaks, the primary peak in 1V/C is preceded by one or two smaller peaks, located at ca. 773 and 738 K. A shoulder peak was also seen in 2V/A (not shown), but in other multiply grafted gels, including 3V/A, only single peaks were observed.

Temperature values T_{max}, corresponding to the temperature of maximum hydrogen consumption, are plotted as a function of coverage in Fig. 3, and data from vanadia

grafted onto pure titania and silica are included. Samples that were multiply grafted show increases in the value of T_{max} with increasing vanadia coverage. Lines drawn through 1–3V/D, 1–3V/A, and 1–3V/H series catalysts have differing slopes and intercepts. Bond and co-workers (*10*) noted similar slope values but different intercepts for pure TiO_2 supports of different origin, and attributed this to differences in surface contamination. Given the magnitude of the spread in T_{max} values, it is unlikely that differences can be solely attributed to experimental handling and impurity levels. The effect of titania content on the T_{max} position is reflected in the differences between the catalyst series 1–3V/A and 1–3V/B. Except for TiO_2 content, both gels were prepared under the same sol-gel preparation conditions, as outlined in the previous sections. T_{max} is lower for the catalysts prepared from gel B, of 1 : 1 Ti : Si ratio, than for any catalysts from gels of 1 : 4 Ti : Si ratio. Furthermore, of all the gel-derived catalysts, it lies the closest to the line representing pure TiO_2-supported vanadia. It is interesting to note also that the slope of the line for 1–3V/A is steeper than for 1–3V/B, yet the intercept values coincide (at zero vanadia coverage).

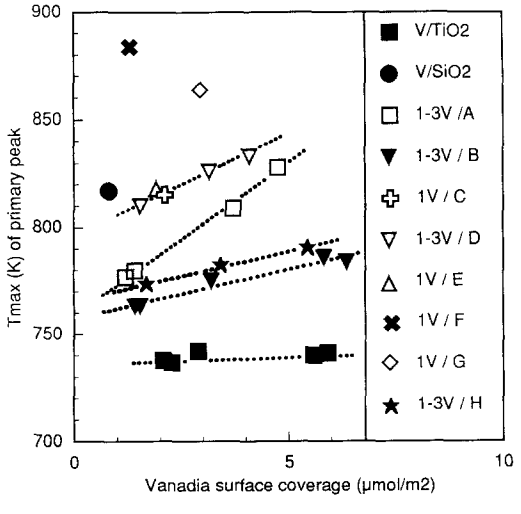

FIG. 3. Temperature of maximum hydrogen consumption, T_{max}, determined by TPR, as a function of vanadia surface density. Data for V/TiO_2 catalysts from Ref. (*11*).

SCR Activity

All catalysts tested for the selective catalytic reduction of NO with NH_3 were highly selective for the reaction:

$$NO + NH_3 + \tfrac{1}{4}O_2 \rightarrow N_2 + \tfrac{3}{2}H_2O$$

A small amount of N_2O was detected at temperatures greater than about 470 K. Arrhenius plots for the activity of singly grafted vanadia on various gel supports are shown in Fig. 4a. The specific activity represents the rate of NO conversion on a per V^{5+} site basis, where the sites are determined from TPR measurements, as described earlier. Note the unusual temperature dependence of the SCR reaction rate for the vanadia grafted on pure silica between 470 and 570 K, which has been observed already in an earlier investigation and has been attributed to the weak vanadia–silica interaction which facilitates changes in the dispersion of the vanadia species under SCR conditions (*3*). This unusual temperature dependence is absent in most of the mixed gel preparations. In catalysts from the amorphous gel supports, 1V/F and 1V/G, a decline in the slope is observed for $T > 470$ K. Also of possible interest are the two points at 510 and 516 K below the activity trend line. This jump is seen also in the NH_3 conversion and N_2 yield, i.e., reaction stoichiometry is maintained, and they may represent an instability behavior as noted with the V-grafted pure silica.

The apparent activation energies have been evaluated for the temperature range 400–470 K. Within 95% confidence limits, E_a values fall in the 40–60 kJ/mol range (Table 2), in agreement with values previously reported in the literature for the dilute gas reaction in the presence of oxygen (*17*). The order of catalyst activity is 1V/H > 1V/C ~ 1V/D > 1V/E ≥ V/Silica > 1V/F > 1V/G.

The kinetic measurements were confirmed to be free of any interparticle mass

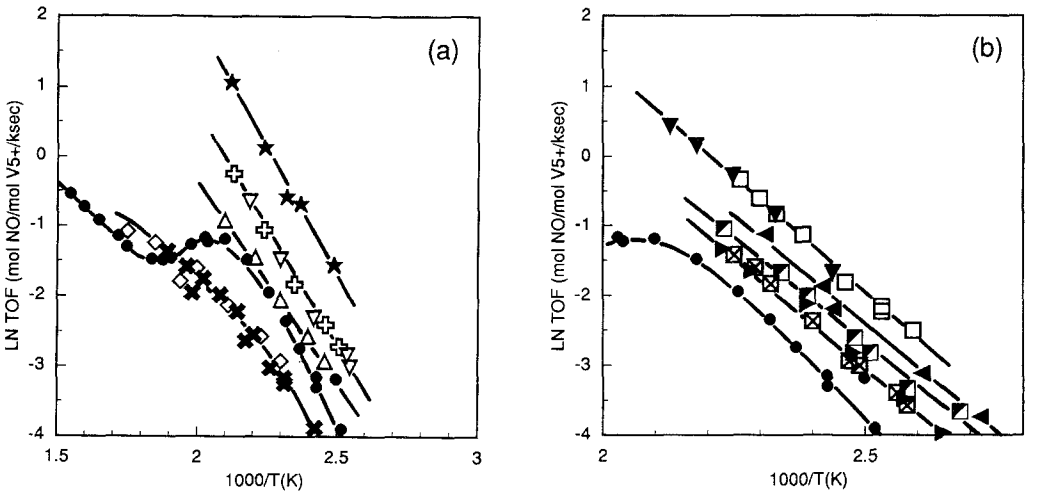

FIG. 4. Arrhenius plots of vanadia-grafted mixed oxide gel catalysts. (a) Singly grafted gels C, D, E, F, G, and H. (b) Multiply grafted gels A and B. Assignments of symbols are given in Table 2. Note enlarged scale of x-axis in Fig. 4a.

transfer limitations. Intraparticle mass transfer influences were found to become relevant only at vanadia loadings higher than those used in the present investigations (*9*).

The SCR behavior of multiply grafted supports was investigated for the series 1–3V/A and 1–3V/B. As shown in Fig. 4b, a decline in specific activity (per V^{5+} site) with each successive grafting is noted in both catalyst series. This indicates that an optimum coverage is achieved already in the first grafting and that subsequent depositions lead to less efficient use of the vanadia either due to lessened accessibility of V^{5+} to reactants or other surface species that may act as a catalyst poison. The reaction mechanism appears to be retained, since the apparent activation energy has not changed with coverage on either support.

Raman Investigations

Figure 5 presents the Raman spectra of catalysts (samples 1–3V/A and 1V/B) prepared according to the method described in Refs. (*3*) and (*12*). The spectrum of catalyst 1V/B (bottom trace) features three strong, narrow bands at 400, 515, and 640 cm^{-1}, which are assigned to well-defined crystallites of anatase (*18*). A weak absorption is noted at 580 cm^{-1}. In the vanadyl stretching region above 1000 cm^{-1} one observes a small peak at 1030 cm^{-1} with a shoulder toward lower frequencies. A broadband around 920 cm^{-1} is of low intensity.

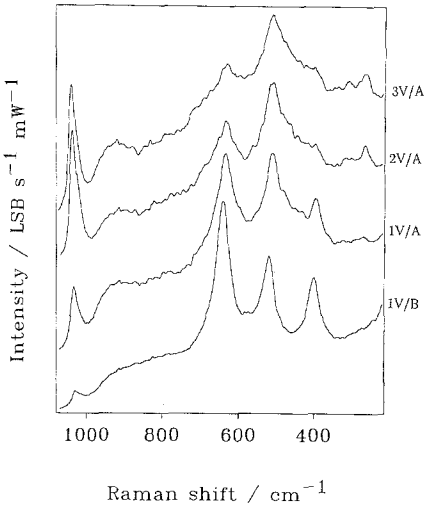

FIG. 5. Raman spectra of vanadia supported on mixed TiO_2–SiO_2 oxide gels A and B, excited by 100 mW of power at 488 nm. Details of measurements are described under the experimental section.

Catalyst 1V/A (second trace) again exhibits bands due to anatase at 400, 515, 640, and 790 cm^{-1} (broad). The presence of minor amounts of rutile can be inferred from a structured band at 440 cm^{-1}, a shoulder at 610 cm^{-1}, and a broad hump at 830 cm^{-1} (*18*). Surface vanadia gives rise to weaker bands at ~700, 570, 485, and 270 cm^{-1} in the region of skeletal motions. Above 800 cm^{-1} we observe a broadband around 920 cm^{-1} and a medium strong peak at 1030 cm^{-1}, with a well discernable shoulder at 1015 cm^{-1}.

In the catalysts 2V/A and 3V/A (third and fourth traces) anatase-related bands are present as well, but they appear decreased in intensity and are gradually becoming broader (3V/A). This broadening is due to the intensification of bands at ~700, 570, and 485 cm^{-1}. Note the intensification of a doublet of bands at 265 and 310 cm^{-1} with increasing coverage. The Raman spectra of catalysts 2V/A and 3V/A are dominated by huge peaks at 1040 cm^{-1}, with an asymmetry toward lower wavenumbers. As compared to sample 1V/A, the broadbands at 920 cm^{-1} appear to be intensified and sharpened.

The influence of *hydrolysis pH* of TEOS (acid or base) is investigated by comparing supports C, D, and E. Common to these materials is that they consist of 20% TiO_2 and 80% SiO_2 and that they have all been prepared by complete hydrolysis of the components. Raman spectra of the singly grafted supports are shown in Fig. 6.

As a reference, the Raman spectrum of an SCR catalyst prepared on a conventional support (threefold VTIP impregnation of TiO_2, P25, Degussa, 50 m^2/g (*11*)) has been included in the bottom trace of Fig. 6. This reference spectrum is dominated by the three absorptions of anatase at 400, 515, and 640 cm^{-1} (*18*). Shoulders at 448 and 610 cm^{-1} are ascribed to the rutile modification of TiO_2, which is present in the P25 support at ~30 wt%. Bands due to surface vanadia are located at 700, 575 (small peak), 495, 265, and 245 cm^{-1}. In the stretching region

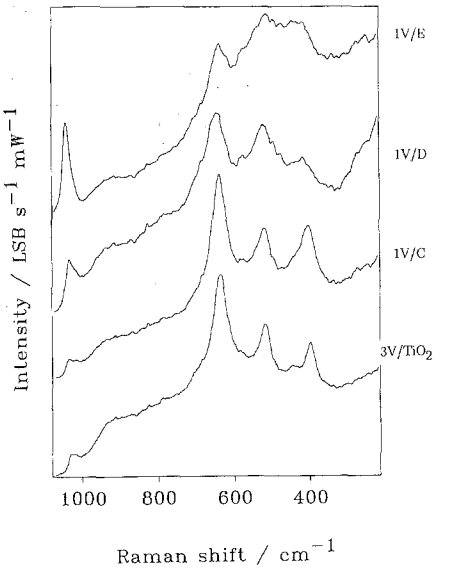

FIG. 6. Raman spectra of vanadia supported on mixed oxide gels C, D, and E. The spectrum of V_2O_5 supported on TiO_2 (P25) is shown in the bottom trace for comparison.

of terminal vanadyl groups (1050–800 cm^{-1}) we note a very broad feature centered at 920 cm^{-1}. A broad hump above 1000 cm^{-1} appears double peaked on close inspection, with maxima at 1030 and 1015 cm^{-1}.

Sample 1V/C (second trace of Fig. 6) strongly resembles a monolayer catalyst on pure TiO_2 (cf. reference spectrum). We observe three strong bands at 640, 512, and 400 cm^{-1} due to well-developed crystallites of anatase. Minor amounts of rutile are indicated by a shoulder at 440 cm^{-1} on the high frequency side of the anatase peak at 400 cm^{-1}. Bands assignable to surface vanadia are found at 700, 580, 270, 245 cm^{-1} (shoulder), and above 800 cm^{-1}. There is a broad feature centered at 915 cm^{-1} and a broadband above 1000 cm^{-1}. Again the latter is double peaked with maxima at 1015 and 1030 cm^{-1}.

Bands due to anatase are less strong and considerably broader in sample 1V/D (third trace from bottom in Fig. 6). In addition to anatase, a shoulder at 610 cm^{-1} and a band at 445 cm^{-1} overlapping with the 400 cm^{-1}

band are proof for the presence of rutile. Further bands in the low wavenumber region are discerned at 700 (sh), 575, 490, 470 cm^{-1} (sh), 265, and 245 cm^{-1}. Again we note a band at 915 cm^{-1}, a medium strong peak at 1030 cm^{-1}, and a shoulder around 1015 cm^{-1}.

Sample E (top trace in Fig. 6) exhibits both features due to anatase (640, 513, 400 cm^{-1}) and rutile (shoulder at 610 and 445 cm^{-1}). Again all TiO_2-related bands are broadened, such that the 400 and 445 cm^{-1} bands overlap strongly. The intensity minimum between the 513 and 445 cm^{-1} support bands appears "filled in" and suggests the presence of a band at ~480 cm^{-1}. Surface vanadia is discerned by shoulders at 700 and 570 cm^{-1}, two weak bands at 270 and 245 cm^{-1}, and a broadband around 920 cm^{-1}, which is more intense as compared to the preceding spectra. A huge peak at 1040 cm^{-1} with a shoulder that dominates the spectrum at 1015 cm^{-1} is also due to a surface vanadia species.

The Raman spectrum of sample 1V/H (Fig. 7) is characterized by the three well-known bands of anatase at 640, 512, and 400 cm^{-1}, indicating that this modification of TiO_2 is exclusively present. Note that no peaks due to rutile are found. In the low-frequency region we observe shoulders at 700, 495, 475, 270, and 245 cm^{-1}, together with a small band at 575 cm^{-1} on the high-frequency edge of the support vibration at 512 cm^{-1}. Above 800 cm^{-1} there is a broadband at 920 cm^{-1} of considerable intensity, followed by a peak at 1030 cm^{-1} with a low-frequency shoulder at 1015 cm^{-1}.

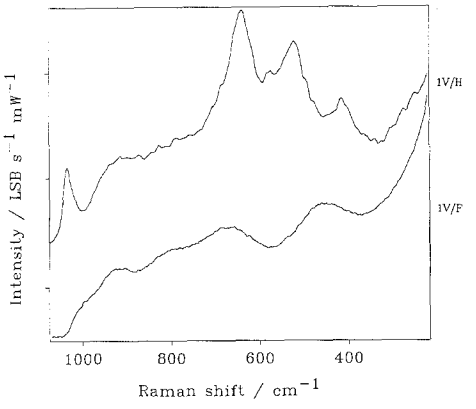

FIG. 7. Raman spectra of vanadia supported on gel F prepared by partial hydrolysis of the respective alkoxide precursors and on support H prepared by coating a dispersion of Aerosil with TIOT (cf. experimental section).

The laser Raman spectrum of a singly grafted catalyst with vanadia supported onto a mixed oxide prepared by *partial* hydrolysis of TEOS in acid is presented in Fig. 7 (sample 1V/F). In contrast to the spectra discussed below, no characteristic Raman bands due to crystallites of anatase or rutile can be detected, in agreement with XRD measurements (*19*). Instead, broadbands at 456 and 800 cm^{-1} are observed which have been assigned (*20*) to stretching and bending vibrations within the silica matrix. An assignment of the two further broadbands at 920 and 670 cm^{-1} are given below.

No useful Raman spectra of sample G have been obtained because of the broadened intense luminenscence background of this sample (*21*). Such behavior has recently been observed with amorphous silica (*22*) and points to the fact that we are encountering a surface that predominantly consists of silica, onto which vanadia is immobilized.

DISCUSSION

Laser Raman Spectroscopy

Before discussing the Raman spectra of singly and multiply grafted mixed oxide carriers presented above, present knowledge on the structure of surface vanadia supported onto SiO_2 and TiO_2 (anatase and rutile, respectively) is summarized. The types and abundance of surface vanadia species depend on surface coverage, nature of oxide support, and the extent of hydration (*11, 21–23*).

Three main classes of surface vanadia species have been characterized on a high-surface-area *silica* support (*24*) under dehydrated conditions. Monomeric and oligomeric species with a tetrahedral coordina-

tion sphere around the central vanadium ion give rise to a narrow V=O stretching absorption at 1040 cm^{-1}. Bands at 920 and 700 cm^{-1} have been assigned (*24*) to two-dimensional vanadia ribbons of finite extent, as found in V_2O_5 gels (*25*). Within these ribbons the vanadium ion is surrounded by five oxygen ligands forming a square pyramid (*25*). An intensive doublet of bands at 667 and 703 cm^{-1} has been associated (*25*) with the stretching motion of oxygen ions in bridging positions between three vanadium centers (OV_3) (*26*).

^{51}V solid state NMR experiments performed under ambient conditions have shown (*27*) that at high surface coverages, vanadium on TiO_2 (anatase) is octahedrally coordinated. The dehydration of a low-coverage catalyst leads to a decrease in the coordination number from 6 to 4. In contrast, the rutile modification of TiO_2 appears to stabilize the fourfold coordination of vanadium(V) oxide up to high surface coverages.

Raman spectroscopic studies (*11, 21–23, 28*) of vanadia supported on TiO_2 (P25, Degussa) have confirmed that under ambient conditions and at low vanadia loadings, a four-coordinate species is formed (*11, 23*). A broad feature is observed (*11, 23*) at 940 cm^{-1}; upon dehydration (*11*) this band disappears, and a small peak at 1030 cm^{-1} is formed. The latter has been assigned (*21, 23, 28*) to a tetrahedral, monomeric species with one terminal, doubly bound oxygen and three oxygen ligands forming bridges to the support. Handy *et al.*(*11*) assign the 1030 cm^{-1} peak to monomeric and oligomeric clusters of vanadia, with one terminal V=O bond and three V—O bonds in bridging position to the support or to other vanadium centers. The latter model agrees with the NMR work of Eckert and Wachs (*27*).

At higher coverages vanadia becomes increasingly sixfold coordinated (*11, 23, 27*). The 940 cm^{-1} band shifts to ~990 cm^{-1} as the vanadia loading is increased. Dehydration removes the broad feature around 990 cm^{-1} and results (*11*) in the appearance of small peaks at 1030, 1015, and 575 cm^{-1}, as well as the formation of broadbands at 920 and 700 cm^{-1}. To illustrate these assignments, the Raman spectrum of a catalyst obtained by threefold impregnation of TiO_2 (P25) (Fig. 6, bottom trace; V^{5+} coverage: 6.1 $\mu mol/m^2$) is analyzed first. The 1030 and 920 cm^{-1} bands are assigned to oligomers and ribbons, as discussed above. The band at 1015 cm^{-1} is attributed (*11*) to the stretching vibration of terminal vanadyl groups within patches of a two-dimensional overlayer. The band at 575 cm^{-1}, which is close in frequency to a band at 530 cm^{-1} in crystalline V_2O_5 and a band at 590 cm^{-1} in the cluster ion $V_{10}O_{26}^{6-}$, corresponds to a stretching motion of oxygen ions in bridging position between three vanadium centers within the layer of these model compounds. The 575 cm^{-1} band parallels the 920 cm^{-1} feature in intensity and has therefore been assigned to the described motion within ribbons or patches of surface vanadia.

This reference information is used to discuss the Raman spectra of Figs. 5–7. Our aim is to clarify how the support composition and structure influence the nature of surface vanadia and the resulting SCR performance. Some of the 20 wt% TiO_2/80 wt% SiO_2 mixed oxides (supports C through G) investigated in this study have recently been characterized by ^{29}Si CP/MAS NMR (*19, 29*) and vibrational spectroscopy (*20*). The results demonstrate that pronounced structural differences exist between the mixed oxides prepared by *partial* and *complete* hydrolysis of the precursor prior to mixing, respectively.

Complete ("single stage") hydrolysis of the alkoxides (TEOS and TIOT, respectively) prior to mixing (*19*) leads to the formation of separate domains of TiO_2 and SiO_2 in the resulting mixed gels. After calcination at 870 K, crystallites of anatase and rutile are embedded into an amorphous silica matrix, as shown by XRD (cf. Table 1). Raman spectra of these 50/50 and 20/80 TiO_2/SiO_2 mixed gels (samples A–E) only feature characteristic vibrations of the anatase or rutile morphology of TiO_2, but *no bands* due to

silica are detected, in accordance with the amorphous structure of this component. It was concluded (*20*) that crystallites of TiO_2 are exposed on the surface of supports A–E.

The Raman spectrum of catalyst 1V/B (bottom trace of Fig. 5) is very similar to the one of vanadia on pure anatase. Note that gel B contains equal fractions of SiO_2 and TiO_2, but with silica again X-ray amorphous. No bands due to rutile are detected. The ability of anatase to stabilize a two-dimensional surface overlayer of vanadia has been emphasized (*30*). Vanadia-related bands at 1030 cm^{-1} (small peak), 920 cm^{-1} (broad), and 580 cm^{-1} are assigned to small clusters and ribbons of limited extent, respectively, which are selectively immobilized on anatase crystallites. No silica-supported vanadia is discerned.

Mixed oxide support A (second to fourth traces in Fig. 5) has been grafted up to three times with VTIP, but precalcination at 870 K was carried out only prior to the first impregnation. Besides Raman bands of anatase, features at 610 cm^{-1} (shoulder) and 440 cm^{-1} indicate that rutile is also exposed on the surface of this catalyst. Interestingly, the V^{5+} coverage, which corresponds to only 1.8 $\mu mol/m^2$ after the first impregnation, increases to 4.5 $\mu mol/m^2$ after the second and 6.0 $\mu mol/m^2$ after the third impregnation. This increasing coverage is clearly reproduced in the Raman spectra: Support-related bands gradually lose intensity, while the surface vanadia-related bands are increasing. In catalyst 1V/A a peak at 1030 cm^{-1} is attributed to small clusters of tetrahedrally coordinated surface vanadia. An intense band around 920 cm^{-1}, together with a small feature around 700 cm^{-1}, indicates a two-dimensional ribbon-like structure, as discussed above. With increasing V^{5+} coverage (1V to 3V) an intensification of bands at 920, 700, 485, 310, and 270 cm^{-1} is noted. Bands at 700, 485, and 310 cm^{-1}, which are also found in the Raman spectrum of crystalline V_2O_5, are assigned (*26*) to the stretching and bending vibrations of oxygen ions between three (OV_3) and two (OV_2) vanadium centers and are characteristic for the layer structure in this oxide. Apparently, with increasing loading the support surface is covered with patches of a two-dimensional overlayer of vanadia. The band at 270 cm^{-1} is assigned to the deformational vibration of terminal vanadyl groups within the layer structure.

Noteworthy changes are occurring in the spectral region above 800 cm^{-1}. The peak at 1030 cm^{-1} in catalyst 1V/A is strongly intensified after two and three impregnations in agreement with the increase in V^{5+} coverage, but appears shifted to 1040 cm^{-1}. We note that the shoulder observed at 1015 cm^{-1} in catalyst 1V/A is no longer present with 2V/A, but both the 1040 and 920 cm^{-1} bands are much narrower than with the singly grafted catalyst. The interpretation of this observation is straightforward with reference to studies of V_2O_5 on silica (*24*). Parallel to the formation of a two-dimensional overlayer on the exposed TiO_2 crystallites, vanadia is successively deposited on the amorphous silica majority component, in the form of small clusters or ribbon-like elements. It therefore appears that vanadia is selectively deposited on anatase/rutile at lower loadings; after covering of the titania sites, vanadia is directed toward energetically less favorable silica sites.

Gel C has been prepared by complete hydrolysis of TEOS in base and of TIOT in acid. Hydrolysis of TEOS in base leads to compact and highly cross-linked clusters of amorphous silica, whereas hydrolysis in an acidic medium tends to produce linear chains with little cross linking. After high-temperature drying of gel C, well-developed crystallites of anatase and rutile are recognized both in XRD (*19*) and in the Raman spectrum (second trace of Fig. 6). For this support a structure has been inferred (*19, 20*) that consists of large domains of crystalline TiO_2 embedded in an amorphous silica matrix. The overall appearance of catalyst 1V/C (second trace in Fig. 6) is indeed very similar to the reference spectrum of $3V/TiO_2$ shown in the bottom trace, which again sug-

gests a preferential deposition of vanadia on TiO_2, with no wetting of silica. Bands at 1015, 920, 700, 575, 485, 270, and 245 cm^{-1} indicate the formation of ribbons and patches of a two-dimensional surface phase, even at the low loading of ~2 $\mu mol/m^2$; this observation demonstrates the high ability of the mixed gel support to stabilize monolayers of dispersed vanadia. A peak at 1030 cm^{-1} indicates, in addition, the presence of smaller entities, i.e., monomers/oligomers with a tetrahedral coordination.

Gels D and E have both been prepared by complete hydrolysis of the two components in acid; gel D was subject to a redispersion treatment in base for 4 days before drying. When dried at low temperature, these gels are X-ray amorphous (*19*), which suggests that hydrolysis of both alkoxides in acid prevents the formation of domains of the two components. After high-temperature drying of gel D, only small domains of anatase were detected in XRD (*19*). Support bands in the third trace of Fig. 6 are much broader than those of sample 1V/C (second trace). In addition to anatase, rutile appears to be present (shoulders at 440 and 610 cm^{-1}). Nevertheless, besides a medium strong peak at 1030 cm^{-1} due to small clusters of vanadia, patches of a two-dimensional overlayer are indicated by bands at 1015 (sh), 920, 700, 575, 490, 470, and 270 cm^{-1}.

Besides crystallites of anatase, up to 30% of rutile has been detected by XRD in the 870 K dried gel E (top trace). The Raman spectrum exhibits bands due to anatase at 640, 515, and 400 cm^{-1}, as well as rutile vibrations at 610 and 440 cm^{-1} (overlapping with the 400 cm^{-1} band). As in the preceding spectrum, patches of a two-dimensional surface phase are inferred from Raman bands at 920, 700, 575, 480, 270, and 245 cm^{-1}. Note that for all catalysts 1V/C,D,E the V^{5+} coverage is about 2 $\mu mol/m^2$. In the vanadyl stretching region, a dominant peak at 1040 cm^{-1} is observed for catalyst 1V/E, in contrast to 1V/C and 1V/D, where it is located at 1030 cm^{-1} with much lower intensity. Based on the arguments presented above it may be proposed that small clusters of vanadia are immobilized on the silica majority fraction of the surface.

The preparation of gel H differs from those previously discussed: a dispersion of Aerosil 200 (Degussa) was mixed with a solution of TIOT prior to hydrolyzing in an acidic medium. Again the Raman spectrum exhibits well resolved, broadened bands of anatase, but not of silica, in agreement with XRD (Table 1). We conclude that this preparation method leads to an encapsulation of the silica globules by a thin layer of anatase. However, in spite of similar coverage, the structure of surface vanadia is different from catalyst 1V/B, for which small vanadia clusters on well-defined anatase crystals have been identified. A strong peak at 1030 cm^{-1} in the Raman spectrum of sample 1V/H is assigned to monomers and oligomers with tetrahedral coordination, located on a thin anatase layer. Bands at 920, 700 (sh), 575, 490, 470, and 270 cm^{-1} demonstrate that also ribbons and patches of a two-dimensional overlayer are stabilized on this surface.

Molecularly mixed solids are approached only when the TIOT component is added after partial (50% on average) hydrolysis of TEOS (two-stage hydrolysis) (*19, 20, 29*). No crystalline domains of TiO_2 have been detected by vibrational spectroscopy or XRD (*19, 20*); rather, vibrational spectroscopy suggests the incorporation of Ti^{4+} cations in tetrahedral coordination into an amorphous silica network. The gels prepared by *partial* hydrolysis exhibit (*20*) a Raman and IR active vibration in the 960- to 940-cm^{-1} range. Huybrechts *et al.* (*31*) have attributed this feature to the vibration of a surface titanyl (Ti=O) group. However, a 960 cm^{-1} band has also been observed in the IR spectrum of crystalline titanium silicalite (*32, 33*) and in IR and Raman spectra of SiO_2—TiO_2 glasses (*34*). In agreement with Refs. (*32–34*), this feature is therefore assigned to a Si—O—Ti stretching vibration; this assignment is supported by the detailed study of Boccuti *et al.* (*33*). The

surface of these supports (samples F, G) mainly consists of amorphous silica, as is readily seen from Fig. 7. Bands that would be typical of anatase or rutile are completely absent in this spectrum. In agreement with the literature (*35*), the very broad bands around 800 and 460 cm^{-1} are assigned to the stretching and bending motions of Si—O—Si bridges in an amorphous silica network. Bands at 920 and 670 cm^{-1} are attributed to two-dimensional ribbons of finite extent. Most interestingly, an inspection of the vanadyl stretching region around 1000 cm^{-1} in Fig. 7 shows the absence of pronounced features, with the exception of a weak and broadband. Note that by comparison with the other catalysts, the bands at 920 and 670 cm^{-1} excel by their high intensity and low width. The implication of this observation is discussed below.

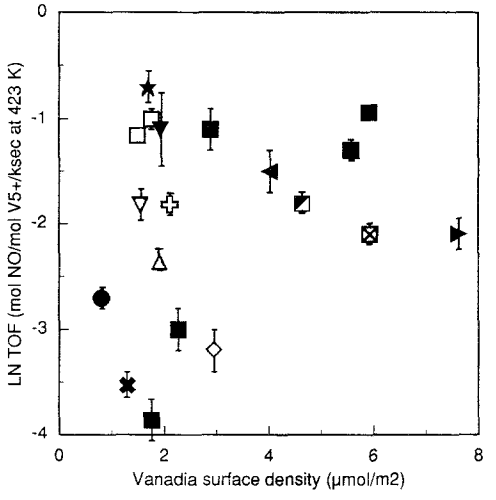

FIG. 8. Plot of NO turnover rate at 423 K as a function of vanadia surface density. Assignments of symbols are given in Table 2. Uncertainty bars were derived from four repetitions of the particular experiment.

SCR Activity, TPR Profiles, and Structural Properties

Under the grafting conditions employed in this study, the multiply grafted catalysts show highest specific activity for the first grafting, and declining activity for the subsequent graftings. The same trend was also observed with pure titania-grafted catalysts (*11*) after coverage had reached a "saturation" level of 4 $\mu mol/m^2$, corresponding to half of the theoretical monolayer defined by Bond *et al.*(*10*). To compare the relative activities of the different catalysts, it therefore appears reasonable to normalize the V^{5+} content of each catalyst with respect to the BET area. The absence of any significant Raman intensity at 996 cm^{-1}, which would be indicative of crystalline V_2O_5, in the Raman spectra of Figs. 5–7 provides evidence that the surface vanadia is disordered and completely dispersed throughout each support material.

NO conversion rates per V(V) site, evaluated at 423 K, are plotted against the V(V) surface density in Fig. 8. It is interesting to note that maximum turnover frequency in the mixed gel catalysts was achieved at a V^{5+} coverage (2 $\mu mol/m^2$), which corresponds to one-half the value found for V/TiO_2 (4 $\mu mol/m^2$) (*11*). Apparently this more efficient use of active material is due to the access and preferential accumulation of vanadia on anatase/rutile crystallites in the gel matrix. In a previous spectroscopic study on the structure of mixed gels C through G (*19, 20*) it was shown that complete hydrolysis of TEOS and TIOT before mixing leads to the formation of crystalline domains of TiO_2 stabilized by an amorphous silica matrix, with the TiO_2 crystallites partly exposed on the surface of the mixed gel (cf. XRD results in Table 1). The similarity of the Raman spectra of our singly grafted mixed oxide carriers (samples A–E and H) with the reference spectrum of a triply grafted pure TiO_2 support (Fig. 6) strongly suggests that vanadia is preferentially immobilized onto surface exposed TiO_2 at low V(V) coverages.

As the coverage is calculated using the nonspecific BET area and it is likely that much of the exposed support surface is actually silica (80 wt% in samples A, C–G), it must be concluded that the "effective" vanadia coverage, assuming it to be associated

with the exposed TiO_2 area, is underestimated. A comparison of our reference spectrum (bottom trace in Fig. 6, 6.1 μmol/m^2) with, e.g., sample 1V/C (second trace in Fig. 6, 2.15 μmol/m^2) suggests an underestimation of the V(V) coverage by a factor of 3. The mixed gel matrix is advantageous, however, in that very small anatase domains are stabilized by the silica, whereas pure anatase normally sinters and, at higher temperatures, converts to the less favorable rutile form.

The dependence of turnover frequency (TOF) on vanadia coverage in mixed gel catalysts is illustrated by the two 1–3V catalyst series tested (Fig. 8). With pure titania-supported vanadia (*11*), TOF increases until a "saturation" level of 4 μmol/m^2 is reached, but stays constant at higher V(V) coverages. However, in both mixed gel catalyst series, TOF is dependent upon vanadia coverage, declining by about threefold with the third grafting (Fig. 8). Since all vanadia loadings correspond to submonolayer amounts (no crystalline or paracrystalline V_2O_5 detected in Raman and XRD), it is doubtful that the TOF decline could be attributed to loss of vanadia accessibility. In several samples, variations in rate are greater than what would be expected solely from differences in coverage. This is particularly true for catalysts that have similar V(V) coverages (e.g., 1V/H vs 1V/C, 1V/D, 1V/E), yet display widely different turnover frequencies. Thus, though the basic reaction mechanism is not modified (E_a is similar for all catalysts, cf. Table 2), the active site is being promoted/inhibited in either a structural or a chemical manner by the nature of the support.

The Raman spectroscopic data of our grafted mixed oxide supports show that the dispersed vanadia may be categorized into three types:

(i) Monomeric and oligomeric species, with a tetrahedral coordination sphere around the central vanadium ion, give rise to a narrow V=O stretching absorption at 1040 cm^{-1} when the cluster is immobilized on SiO_2, which is shifted to 1030 cm^{-1} when the support is TiO_2.

(ii) Semi-infinite "ribbons," in which the vanadium ion is in the center of a square pyramid, are recognized by Raman bands at 920, 680, and 575 cm^{-1}.

(iii) In two-dimensional patch structures, the local environment of vanadium resembles the structure of layers in crystalline V_2O_5, but is more strongly associated with the support, as has been previously reported for titania-supported vanadia (*36*). The patchy layers consist of vanadium centers surrounded by five oxygen ions in a square pyramidal geometry, with a sixth oxygen ligand in bridging position to the support. Observed bands at 700, 485, 310, and 245 cm^{-1} are assigned to the stretching and bending vibrations of oxygen ions bridging two or three vanadium centers within a layer, in accordance with the Raman spectrum of V_2O_5 (*26*). A peak at 1015 cm^{-1} and a band at 270 cm^{-1} are attributed to the stretching and bending vibrations of terminal V=O groups in these two-dimensional surface species.

TABLE 2

Apparent Activation Energies for SCR of Vanadia Grafted on TiO_2–SiO_2 Mixed Oxide Gels

Plot symbol	Catalyst	E_a (kJ/mol)
■	V/TiO_2	60 ± 8
●	1V/SiO_2	60 ± 5
□	1V/A	56 ± 3
◩	2V/A	50 ± 4
⊠	3V/A	55 ± 2
▼	1V/B	57 ± 6
◀	2B/B	52 ± 9
▶	3V/B	53 ± 6
✞	1V/C	53 ± 7
▽	1V/D	52 ± 10
△	1V/E	47 ± 4
✖	1V/F	46 ± 6
◇	1V/G	35
★	1V/H	59 ± 11

Note. Plot symbols refer to Figs. 4a, 4b, 8, and 9.

Inspection of the Raman spectra in Figs. 5–7 reveals that, except for catalyst 1V/F, all mentioned species, i.e., clusters, ribbons, and patches, can be detected on each of our mixed oxide carriers. However, it is noted that the shapes of surface vanadia related bands are subject to variations on the differently prepared mixed oxide supports.

At this point it is convenient to define the terms of silica-like and titania-like behavior, as limiting cases for the classification of our catalysts. A silica-like behavior is characterized by fairly weak bonding between the silica support and the immobilized metal oxide species. As a consequence, even at low-coverage formation of crystalline V_2O_5 has been observed (*37*). In contrast, the vanadia–titania interaction has been established to be very strong.

From the spectroscopic information, the two limiting cases are readily discerned. Two characteristic features are identified for vanadia–silica catalysts (*24*): (i) The value of the stretching frequency of terminal vanadyl bonds observed on silica at 1040 cm^{-1} is the highest among a series of supports (e.g., SiO_2, TiO_2, Al_2O_3, SiO_2/TiO_2). This has been attributed (*24, 28*) to a difference in vanadyl bond order, which measures the strength of interaction with the respective support. (ii) All vanadia-related bands on silica excel by a relatively narrow band width, again attributed (*24*) to a weaker interaction of vanadia with the support. As a consequence of this weak interaction, it was established (*24*) that no compact two-dimensional overlayer can be achieved on silica. In summary, a strong narrow band at 1040 cm^{-1} (small clusters) and a narrow feature at 920 cm^{-1} (ribbons of limited extent) are an indication of silica-like behavior. The vanadia sites in V/silica are about fivefold less active than V/TiO_2 and also show an instability in the Arrhenius plot between 463 and 512 K, which is nonexistent in V/TiO_2 (cf. Figs. 4a and 4b). No crystalline phases have been detected with our submonolayer vanadia-grafted silica catalyst (*24*). The unusual temperature dependence of the SCR activity of this type of catalyst in the 470–570 K range has been explained by an agglomeration/redispersion phenomenon (*3*). Approaching the onset of instability from low temperatures, the weakly bound vanadia ribbon structure may find more stability in an agglomerated form in which the vanadia is less accessible. Above the instability region, the vanadia may redisperse if the oxide–oxide interaction becomes more favorable.

The characteristic Raman spectroscopic features of a titania-like catalyst are depicted in the bottom trace of Fig. 6. As compared to vanadia–silica, all bands are considerably broader (see 920 cm^{-1} feature). The peak indicating small clusters of vanadia is of much lower intensity and appears downshifted to 1030 cm^{-1}. A second weak maximum at 1015 cm^{-1} and a shoulder at 700 cm^{-1} prove the presence of patches of a two-dimensional overlayer.

On the basis of these characteristics of titania- and silica-supported vanadia, the catalysts investigated in Figs. 5 and 6 are tentatively assigned to the two categories. Catalysts 1V/B and 1V/C are easily identified as titania-like, as revealed by a comparison with the reference spectrum (bottom trace in Fig. 6). This behavior points to the presence of extended, well-defined crystallites of TiO_2 on the surface of mixed oxides B and C, where vanadia is stabilized in the same way as on pure titania. Note, however, that the structure of surface vanadia is somewhat different on the two oxides, although the V^{5+} coverage is nearly identical ($\sim 2\ \mu mol/m^2$). On 1V/B small clusters (1030 cm^{-1} band) and ribbons (broad 920 cm^{-1} band) are detected as on V/TiO_2 catalysts at low loadings (*11*). On the other hand, catalyst 1V/C is more similar to a V/TiO_2 catalyst at higher loads (e.g., our reference catalyst $3V/TiO_2$, Fig. 6, with a coverage of 6.1 $\mu mol/m^2$). This appears to indicate a lower capacity of support C to immobilize vanadia onto TiO_2, which is probably due to a smaller extent of the anatase particles.

Nearly perfect silica-like behavior is en-

countered with catalysts 2V/A, 3V/A, and 1V/E. For series A it has been stated above that well-defined crystallites of TiO_2 are observed on the surface. However, *at high loadings* (4.8 and 6.0 μmol/m^2) the energetically favorable anatase sites are covered, and vanadia is directed toward less favorable silica sites. This development is well recognized in our Raman spectra: Intensive, narrow bands are developing at 1040 and 920 cm^{-1}, which are typical for silica-supported vanadia. We also note that the relative abundance of the different surface species is heavily influenced by the support. Although bands at 700, 485, and 270 cm^{-1} indicate the formation of VO_x patches, spectra 2V/A and 3V/A are dominated by a peak at 1040 cm^{-1} (clusters) and a relatively narrow band at 920 cm^{-1} (ribbons), which reflects the inability of silica to stabilize extended two-dimensional overlayers.

Catalyst 1V/E exhibits a peak at 1040 cm^{-1} indicating silica-bound vanadia clusters, but in contrast to, e.g., 3V/A the band at 920 cm^{-1} is very broad, as in the titania-like catalyst 1V/C. From the observation that titania-related bands are relatively broad in catalysts 1V/E and 1V/D, it was concluded above that the anatase domains are small. In addition, bands at 610 and 440 cm^{-1} indicate considerable amounts of rutile, which is characterized by a surface area five times lower than that of anatase. It may therefore be argued that the small domains of TiO_2 exposed on the surface are readily covered with patchy and/or ribbon-like two-dimensional overlayers and that the excess vanadia is stabilized on silica sites in the form of small clusters of tetrahedral symmetry.

A behavior that is intermediate between silica- and titania-like is noted for catalysts 1V/D and 1V/A. For gel D, the percentage of rutile is smaller than with support E. The loading of 1V/D is 0.2 μmol/m^2 less than on catalyst 1V/E and 0.3 μmol/m^2 higher than on 1V/C; the Raman spectrum of this catalyst appears to represent an intermediate state between the two extremes. A peak at 1015 cm^{-1}, a broadband at 920 cm^{-1}, and features at 700, 580, 490, 470, and 270 cm^{-1} indicate titania-like patches and ribbons; however, the peak at 1030 cm^{-1} is much more intense than that on catalyst 1V/C and suggests that small clusters of vanadia deposited on TiO_2 are chemically influenced by neighboring silica sites. This also holds true for catalyst 1V/A, where band positions match vanadia on titania, but the relative abundance of the features is closer to the one found on silica. It is likely that in catalysts 1V/D and 1V/A vanadia covers both titania and silica sites, resulting in an intermediate behavior.

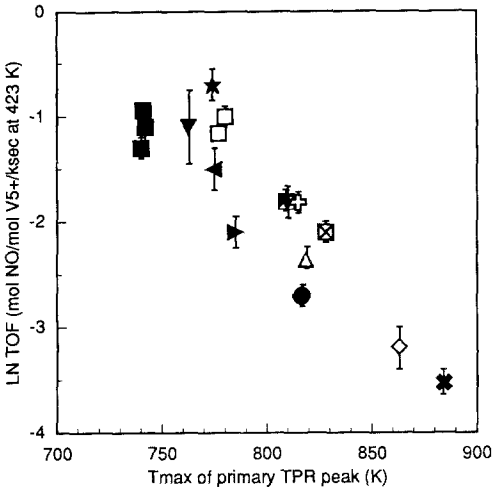

FIG. 9. Correlation between NO turnover rate at 423 K and the location of T_{max} from TPR. Plot symbols are the same as those in Fig. 3. Assignments of symbols are given in Table 2.

Complementary to the Raman spectroscopic experiments, a clear measure of the variation of the dispersed vanadia phase among supports is provided by the TPR behavior. Shown in Fig. 9 is a plot, for all catalysts, of the NO turnover rate per V(V) site as a function of the TPR parameter T_{max}. The summarizing plot shows a general trend of decreasing TOF with increasing temperature of vanadia reduction. Since the vanadia must be labile to perform the necessary redox cycle, a greater ease of reduction would

promote this aspect of the mechanism. The similarity of the Arrhenius data hints to active sites of similar structure on all catalysts.

The classification of the catalysts into silica-like, titania-like, and intermediate behavior will now be correlated with their temperature of maximum reduction rate, T_{max} (Fig. 9). As a reference, a singly grafted SiO_2 carrier is characterized by a T_{max} value of 820 K (cf. Table 1), whereas vanadia on titania is reduced at much lower temperatures, in the range from 730 to 740 K (*8, 9, 11*). The silica-like catalysts 3V/A and 1V/E indeed exhibit T_{max} values of 828 (822) and 820 K, i.e., very similar to V/SiO_2. The classification of catalyst 1V/B as titania-like is confirmed by the low T_{max} value of 763 K.

Sample 1V/C exhibits spectral similarities with V/TiO_2, in agreement with two low-temperature shoulders in the reduction peak at 773 and 738 K. However, the main TPR maximum for catalyst 1V/C is located at 815 K. No indications of intermediate behavior were found in our Raman spectrum. Intermediate reduction behavior is noted for catalysts 1V/A, 2V/A, and 1V/D, which exhibit T_{max} values around 810 K. At least for catalysts 1V/A and 1V/D, intermediate behavior has also been inferred from Raman spectroscopy.

In summary, catalysts that exhibit high activities per site (TOF) evidently coincide with the most easily reducible forms of vanadia in Fig. 9 (catalysts 1V/B, 1V/H, 1V/A, and 2V/B). These samples include the vanadia/anatase type (1V/B, 2V/B, 1V/H), but also intermediate structures (1V/A). On the other hand, it is easily recognized that silica-like behavior coincides with T_{max} values of about 820 K.

Catalysts prepared from gels A, B, C, D, E, and H show activities (cf. Figs. 4a, 4b) higher than V/SiO_2 and no evidence of instability. Common to all these gels is their content of anatase crystallites. Nevertheless these catalysts exhibit SCR activities characteristic or even better than titania-supported vanadia. The reason may be found in the limited extent of our two-dimensional ribbons and/or patches, which are locally very similar to the layers of crystalline V_2O_5. Therefore, the vanadia surface species may be immobilized on anatase in a preferred orientation, such that the short-range order is similar to that of the (010) V_2O_5 face. It should be noted, however, that sites on the (010) face are not necessarily responsible for SCR activity (*39*).

Next, we comment on the difference noted in Fig. 3 between catalyst series 1–3V/A and 1–3V/B. It is observed that the increase of T_{max} with V(V) coverage is much higher for the A series than for the B series. This behavior is due to two reasons. (i) Gel B is a mixed oxide containing equal amounts of SiO_2 and TiO_2, and therefore should expose a higher area of TiO_2 as compared to the 20% TiO_2/80% SiO_2 gel A. (ii) The Raman spectrum of catalyst 1V/B reveals well-crystalline anatase particles in the support, whereas in gel A rutile is found as well. In summary, the differences noted between series A and B are due to (i) the higher capacity of gel B to stabilize surface vanadia and (ii) the abundance of energetically favorable anatase sites on support B. Note that on catalyst 1V/B, no patches of a two-dimensional overlayer are found, such as on a low-coverage V/TiO_2 catalyst. This suggests that the capacity of the anatase domains in the dispersed gel B to immobilize vanadia is higher than the one of pure titania (P25).

The mixed gel catalyst 1V/H performs as well or better than V/TiO_2. Electron micrographs of the calcined gel H showed that its pore volume is formed by the gaps between the nonporous globules of Aerosil powder that had been coated with a titania outer layer. X-ray and electron diffraction patterns indicated the presence of small or poorly crystalline anatase. In accordance with these findings, the Raman spectrum of 1V/H exhibits only bands due to anatase, but not of rutile. The width of these bands documents the poor crystallinity of this modification. The structure of surface vanadia on this support is again heteroge-

neous. Besides small clusters of tetrahedral symmetry, ribbons and patches of a two-dimensional surface phase are present (bands at 920, 700, 580, 490, 470, 270, 245 cm^{-1}). However, although the position of main vanadia features at 1030 and 920 cm^{-1} suggest titania-like behavior, the relative intensities and widths of these bands are similar to catalyst 1V/A, for which an intermediate behavior between the two limiting cases has been found. In agreement with this classification, the surface vanadia species grafted onto support H are less reducible than those on pure titania: T_{max} for 1V/H lies about midway between the values observed for a vanadia layer of the same coverage on pure silica and on pure titania, respectively

$$\{V/TiO_2,\ T_{max} = 740\ K;\ 1\ V/H,\ T_{max} = 774\ K;\ 1\ V/A,\ T_{max} = 780\ K\}.$$

Interestingly, the trend of T_{max} with increasing vanadia coverage (Fig. 3) for gel H is more similar to vanadia supported on gel B (Ti/Si = 1 : 1) than on gel A, which exhibits a steeper slope. Like gel B, the support H appears to possess a high surface area capable of immobilizing vanadia on the energetically more favorable anatase surface. However, the differences between gels H and B with respect to surface vanadia structure and T_{max} values (1V/B, T_{max} = 763 K) strongly suggest that on support H, the vanadia is being influenced by a silica interaction. The latter could be due to exposed silica surface areas neighboring the vanadia/anatase interface. Alternatively, if a thin anatase layer were to encapsulate the silica globules completely, one could consider that the anatase microcrystallites are perturbed and, consequently, the anatase/vanadia interface structure was altered. From the Raman spectroscopic results, the latter possibility is unlikely, as the three main vibrations of the anatase bulk structure are well developed in the spectrum.

Clearly, the catalysts 1V/F and 1V/G exhibit behavior that resembles V/silica, as expressed by the high temperature of TPR peaks, low specific activities in SCR compared to V/TiO_2 catalysts, and changes in slope noted in the Arrhenius plots at higher temperatures. The gels are amorphous; ^{29}Si solid state NMR results show (*19, 29*) that there is some degree of molecular mixing. This result has recently been confirmed by vibrational spectroscopy (*20*). In contrast to completely hydrolyzed mixed gels, no Raman bands due to TiO_2 have been detected in the two-stage hydrolyzed gels. Very broad bands around 450 and 800 cm^{-1} are assigned (*20*) to the stretching and bending vibrations of an amorphous silica network. Diffuse reflectance FTIR spectra of gels F and G exhibit a dominant band at 960 cm^{-1}, which has been attributed (*32–34*) to the vibrations of Si—O—Ti structural elements, and proves that Ti^{4+} cations are incorporated into the amorphous silica network in a tetrahedral environment (*32–34*).

Most noteworthy are the Raman spectroscopic results on the structure of surface vanadia deposited on gel F. In our previous study on the structure of surface vanadia on a high-surface-area silica support (*24*), only small clusters of tetrahedrally coordinated vanadium were detected at very low loadings discerned by a peak at 1040 cm^{-1}. With higher coverages an intensification of the 1040 cm^{-1} peak is paralleled by the appearance of bands around 920 and 700 cm^{-1}, which are assigned to ribbons of limited lateral extent and indicate the higher aggregated form of vanadia (V^V ions in the center of a square pyramid). Surprisingly, gel F apparently does not have the capability of stabilizing vanadia clusters of low molecular weight. Instead, narrow and intense bands at 920 and 670 cm^{-1} are formed exclusively. At this point it must be emphasized that the intensity and narrowness of these features is unique and has not been observed with either pure silica or silica-like mixed gels. It was emphasized (*24*) that the intensity and narrowness of the 920 and 670 cm^{-1} features can serve as an indicator for a weak interaction of dispersed vanadia with the respective

support; this conclusion was derived from a comparison of Raman spectra on vanadia/silica and on vanadia/mixed oxide supports.

We conclude that the amorphous silica surface of gel F is incapable of stabilizing a thin vanadia layer and exhibits less favorable properties than V/SiO_2. This is documented by several points. (i) The T_{max} value of 884 K is ~60 K higher than observed for V/SiO_2. (ii) The turnover frequency as a function of V(V) coverage is less than determined on V/SiO_2 (cf. Fig. 8). (iii) The amorphous silica surface is incapable of dispersing and stabilizing small clusters of vanadia, as indicated by the lack of a band at 1040 cm^{-1} in the Raman spectrum. (iv) A ribbon structure of limited lateral extent is found that exhibits an extraordinarily weak interaction with the silica surface, as indicated by the width of the 920 and 670 cm^{-1} bands. The latter resemble the bands in spectra of pure V_2O_5 gels, reported by Abello *et al.* (*25*), where no supporting medium was involved.

CONCLUSIONS

Vanadia supported on TiO_2–SiO_2 mixed oxide gels yields highly active and stable catalysts for the catalytic reduction of NO with NH_3, provided that the titania is present in partly crystalline form of anatase and possibly rutile, in which case the catalysts exhibit behavior characteristic of V/TiO_2. Vanadia is less active and stable on amorphous supports, where it displays turnover frequencies lower than those on pure silica and dropoff in the Arrhenius plot for $T \geq 470$ K. Correlating turnover data with the primary TPR peak temperature demonstrates that less reducible forms of the dispersed vanadia phase (V/SiO_2 type) are less active for SCR. The more easily reducible forms are assigned to the V/TiO_2 type. The reducibility of the dispersed vanadia phase can be influenced by varying the microstructure of a given support composition, which has implications on the activity of vanadia catalysts for SCR.

Neither multilayers nor crystalline aggregates of V_2O_5 are produced by the present grafting technique based on the immobilization of vanadyl triisopropoxide. The position and width of vanadia-related Raman bands can be used to discriminate whether the deposition of vanadia is realized on silica or titania. An intermediate behavior can be observed when patches of vanadia extend from crystalline TiO_2 domains onto the surrounding silica matrix. Upon immobilization, vanadia tends to cover first the exposed titania faces, before deposition on silica where the interaction is weaker.

Single-stage hydrolyzed TiO_2–SiO_2 gels are found to contain TiO_2 crystallites. The anatase domains are large when the TEOS component is hydrolyzed under basic conditions leading to silica clusters. These samples have a high capacity of stabilizing two-dimensional overlayers of vanadia. In contrast, TiO_2 domains are small when acid conditions are used in TEOS hydrolysis. These supports exhibit a considerably lower ability to host vanadia layers, and the influence of the silica component is more pronounced.

Two-stage hydrolyzed gels exhibit a morphology characterized by a core containing mainly titania, which is surrounded by a shell consisting of amorphous silica. This surface is incapable of stabilizing vanadia in a form suitable for SCR.

The catalytic behavior of the vanadia species supported on the TiO_2–SiO_2 mixed oxides is shown to be correlated with their ease of reduction, as measured by the temperature of maximum hydrogen consumption in temperature-programmed reduction.

ACKNOWLEDGMENTS

Assistance by E. Curry-Hyde with the collection of mass spectroscopic data is gratefully acknowledged. This work has been supported by grants from the Schweizerische Nationalfonds (NFP 24) and the Deutsche Forschungsgemeinschaft (SFB 213).

REFERENCES

1. Bosch, H., and Janssen, F., *Catal. Today* **2**(4), (1988).

2. Shikada, T., Fujimoto, K., Kunugi, T., and Tominaga, H., *J. Chem. Technol. Biotechnol. A* **33,** 446 (1983).
3. Baiker, A., Dollenmeier, P., Glinski, M., and Reller, A., *Appl. Catal.* **35,** 365 (1987).
4. Odenbrand, C. U. I., Lundin, S. T., and Andersson, L. A. H., *Appl. Catal.* **18,** 335 (1985).
5. Shikada, T., Fujimoto, K., Kunugi, T., and Tominaga, H., *Ind. Eng. Chem. Prod. Res. Dev.* **20,** 91 (1981).
6. Vogt, E. T. C., Boot, A., van Dillen, A. J., Geus, J. W., Janssen, F. J. J. G., and van den Kerkhof, F. M. G., *J. Catal.* **114,** 313 (1982).
7. Bond, G. C., and Flamerz, S., *Appl. Catal.* **71,** 1 (1991).
8. Kijenski, J., Baiker, A., Glinski, M., Dollenmeier, P., and Wokaun, A., *J. Catal.* **101,** 1 (1986).
9. Baiker, A., Dollenmeier, P., Glinski, M., and Reller, A., *Appl. Catal.* **35,** 351 (1987).
10. Bond, G. C., Zurita, J. P., Flamerz, S., Gellings, P. J., Bosch, H., van Ommen, J. G., and Kip, B. J., *Appl. Catal.* **22,** 361 (1986).
11. Handy, B. E., Gorzkowska, I., Nickl, J., Baiker, A., Schraml-Marth, M., and Wokaun, A., submitted for publication.
12. Handy, B. E., Maciejewski, M., Baiker, A., and Wokaun, A., submitted for publication.
13. Stencel, J. M., Makovsky, L. E., Sarkus, T. A., De Vries, J., Thomas, R., and Moulijn, J. A., *J. Catal.* **90,** 314 (1984); Stencel, J. M., Makovsky, L. E., Diehl, J. R., and Sarkus, T. A., *J. Raman Spectrosc.* **15,** 282 (1984).
14. Payen, E., Kasztelan, S., Grimblot, J., and Bonnelle, J. P., *J. Raman Spectrosc.* **17,** 233 (1986).
15. Schraml-Marth, M., Wokaun, A., and Baiker, A., *J. Catal.* **124,** 86 (1990).
16. Curry-Hyde, E., and Baiker, A., *Ind. Eng. Chem. Res.* **29,** 1985 (1990).
17. Inomata, M., Miyamoto, A., Ui, T., Kobayashi, K., and Murakami, Y., *Ind. Eng. Chem. Prod. Res. Dev.* **21,** 424 (1982).
18. Beattie, I. R., and Gilson, T. R., *Proc. Roy. Soc. A* **307,** 407 (1968).
19. Handy, B. E., Baiker, A., Walther, K.-L., and Wokaun, A., *in* "Synthesis and Preparation of Catalysts" (E. W. Corcoran and M. J. Ledoux, Eds.), p. 107. Materials Research Society, 1990.
20. Schraml-Marth, M., Walther, K. L., Wokaun, A., and Baiker, A., *J. Non-Cryst. Solids,* in press.
21. Wachs, I. E., *J. Catal.* **124,** 570 (1990).
22. Cristiani, C., Forzatti, P., and Busca, G., *J. Catal.* **116,** 568 (1989); Ramis, G., Cristiani, C., Forzatti, P., and Busca, G., *J. Catal.***124,** 574 (1990).
23. Wachs, I. E., Jehng, J.-M., and Hardcastle, F. D., *Solid State Ionics* **32/33,** 904 (1989).
24. Schraml-Marth, M., Wokaun, A., Pohl, M., and Krauss, H. L., *J. Chem. Soc., Faraday Trans.,* **87,** 2635 (1991).
25. Abello, L., Husson, E., Repelin, Y., and Lucazeau, G., *J. Solid State Chem.* **56,** 379 (1985).
26. Beattie, I. R., and Gilson, T. R., *J. Chem. Soc. A,* 2322 (1969).
27. Eckert, H., and Wachs, I. E., *Mater. Res. Soc. Symp. Proc.* **111,** 459 (1988); Eckert, H., and Wachs, I. E., *J. Phys. Chem.* **93,** 6796 (1989).
28. Went, G. T., Oyama, S. T., and Bell, A. T., *J. Phys. Chem.* **94,** 4240 (1990).
29. Walther, K.-L., Wokaun, A., and Baiker, A., *J. Non-Cryst. Solids,* **34,** 47 (1991).
30. Eckert, H., Deo, G., Wachs, I. E., and Hirt, A. M., *Colloids Surf.* **45,** 347 (1990).
31. Huybrechts, D. R. C., de Bruycker, L., and Jacobs, P. A., *Nature* **345,** 240 (1990).
32. Taramasso, M., Perego, G., and Notari, B., U.S. patent 4.410.501.
33. Boccuti, M. R., Rao, K. M., Zecchina, A., Leofanti, G., and Petrini, G., *in* "Structure and Reactivity of Surfaces" (C. Morterra, A. Zecchina, and G. Costa, Eds.), p. 133. Elsevier, Amsterdam, 1989.
34. Görlich, E., Blaszczak, K., Stoch, A., and Sieminska, G., *Mater. Chem.* **5,** 289 (1980); Brest, M. F., and Condrate, R. A., *J. Mater. Sci. Lett.* **4,** 994 (1985).
35. Bates, J. B., *J. Phys. Chem.* **57,** 4042 (1972); Etchepare, J., Mezianant, M., and Kaplan, P., *J. Phys. Chem.* **68,** 1531 (1978).
36. Schraml, M., Fluhr, W., Wokaun, A., and Baiker, A., *Ber. Bunsenges. Phys. Chem.* **93,** 852 (1989).
37. Roozeboom, F., Mittelmeijer-Hazeleger, M. C., Moulijn, J. A., Medema, J., de Beer, V. H. J., and Gellings, P. J., *J. Phys. Chem.* **84,** 2783 (1980).
38. Griffith, W. P., and Wickins, F. D., *J. Chem. Soc. A,* 1087 (1966).
39. Gasior, M., Haber, J., Machej, T., and Czeppe, T., *J. Mol. Catal.***43,** 359 (1988).